SHOCK, Vol. 36, No. 2, pp. 128 137, 2011

WOOD BARK SMOKE INDUCES LUNG AND PLEURAL PLASMINOGEN ACTIVATOR INHIBITOR 1 AND STABILIZES ITS mRNA IN PORCINE LUNG CELLS

Krishna K. Midde,* Andriy I. Batchinsky,† Leopoldo C. Cancio,† Sreerama Shetty,* Andrey A. Komissarov,* Galina Florova,* Kerfoot P. Walker III,† Kathy Koenig,* Zissis C. Chroneos,‡ Tim Allen,§ Kevin Chung,† Michael Dubick,† and Steven Idell*

**The Texas Lung Injury Institute, The University of Texas Health Science Center at Tyler; †US Army Institute of Surgical Research, Fort Sam, Houston; and Departments of ‡Biochemistry and §Pathology, The University of Texas Health Science Center at Tyler, Tyler, Texas*

Received 24 Jan 2011; first review completed 4 Feb 2011; accepted in final form 24 Mar 2011

ABSTRACT Although aberrant fibrinolysis and plasminogen activator inhibitor 1 (PAI-1) are implicated in acute lung injury, the role of this serpin in the pathogenesis of wood bark smoke (WBS) induced acute lung injury (SIALI) and its regulation in resident lung cells after exposure to smoke are unclear. A total of 22 mechanically ventilated pigs were included in this study. Immunohistochemical analyses were used to assess fibrin and PAI-1 in the lungs of pigs with SIALI *in situ*. Plasminogen activator inhibitor 1 was measured in bronchoalveolar lavage fluids by Western blotting. Induction of PAI-1 was determined at the protein and mRNA levels by Western and polymerase chain reaction analyses in primary porcine alveolar type II cells, fibroblasts, and pleural mesothelial cells. Plasminogen activator inhibitor 1 mRNA stability was determined by transcription chase studies. Gel shift analyses were used to characterize the mechanism regulating PAI-1 mRNA stability. Smoke-induced ALI induced PAI-1, with prominent extravascular fibrin deposition in large and small airways as well as alveolar and subpleural compartments. In pleural mesothelial cells, lung fibroblasts, and alveolar type II cells, PAI-1 mRNA was stabilized by WBS extract and contributed to induction of PAI-1. The mechanism involves dissociation of a novel 6-phospho-D-gluconate-NADP oxidoreductase like PAI-1 mRNA binding protein from PAI-1 mRNA. Exposure to WBS induces prominent airway and mesothelial expression of PAI-1, associated with florid distribution of fibrin in SIALI *in vivo* Wood bark smoke components induce PAI-1 *in vitro* in part by stabilization of PAI-1 mRNA, a newly recognized pathway that may promote extravascular fibrin deposition and lung dysfunction in SIALI.

KEYWORDS Acute lung injury, fibrin, fibrinolysis, serpin, smoke inhalation

ABBREVIATIONS 3′ UTR 3′ Untranslated region; 6-PGD 6-phospho-D-gluconate-NADP oxidoreductase; ARDS Acute respiratory distress syndrome; APRV Airway-pressure-release ventilation; ATII Alveolar type II cells; AU Arbitrary fluorescence emission units; BAL Bronchoalveolar lavage; BALF BAL fluid; CMV Conventional mechanical ventilation; F_{IO_2} Fraction of inspired oxygen; HBSS Hanks balanced salt solution; ICU Intensive care unit; PBS Phosphate-buffered saline; PL Plasmin; PGN Plasminogen; PA PGN activator; PAI-1 Plasminogen activator inhibitor 1; PMCs Pleural mesothelial cells; PEEP Positive end-expiratory pressure; Pa_{CO_2} Partial pressure of carbon dioxide in arterial blood; Pa_{O_2} Partial pressure of oxygen in arterial blood; PIP Peak inspiratory pressure; PFs Pleural fluids; PFR Pa_{O_2}-to-F_{IO_2} ratio; scuPA Single-chain urokinase; SIALI Smoke-induced acute lung injury; TV tidal volume; uPA Urokinase-type plasminogen activator; WBSE Wood bark smoke extract

INTRODUCTION

Smoke inhalation injury occurs in 5% to 15% of patients currently admitted to US burn centers, and greatly increases postburn morbidity and mortality (1). The pathogenesis of smoke inhalation–induced acute lung injury (SIALI) involves activation of a number of proinflammatory cascades, leading to disordered coagulation and perturbed fibrinolysis. In particular, derangements of these pathways have been strongly implicated in abnormal extravascular fibrin turnover (1, 2). Fibrin deposition in the small airways, in combination with airway hyperreactivity, has been associated with respiratory dysfunction and obstruction in SIALI (2). These observations provide a strong rationale for therapy targeting disordered fibrin turnover in this setting, and inhalational anticoagulant and fibrinolytic interventions have been successfully used to ameliorate lung dysfunction in SIALI in animal models (3–5).

Disordered fibrin turnover in the lung in patients with acute lung injury (ALI) and acute respiratory distress syndrome (ARDS) is consistently associated with a profound local defect in fibrinolytic activity. As measured in bronchoalveolar lavage (BAL) fluid, this defect in fibrinolysis is mainly attributable to overexpression of plasminogen activator inhibitor 1 (PAI-1) (6, 7). In the lung, PAI-1 not only regulates alveolar proteolysis, but also participates in cellular signaling and regulates airway and alveolar injury and repair (8). Increased expression of PAI-1 (or homozygosity for the PAI-1 4G allele) is associated with poor outcomes in patients with ALI (9–11). Elevated plasma PAI-1 levels have also been reported in 15 patients with burn and inhalation injury (12). However, understanding of the role

Address reprint requests to Steven Idell, MD, PhD, The University of Texas Health Science Center at Tyler, Laboratory C-6, Routes 271 and 155, Tyler, TX 75708. E-mail: steven.idell@uthct.edu.

This study was supported by the National Institutes of Health (NHLBI PPG PO1 HL076406, R-21-HL093547, FAMRI-ID-082380), the Texas Lung Injury Institute, and the Combat Critical Care Engineering task area, Combat Casualty Care Research Program, US Army Medical Research and Materiel Command.

The opinions or assertions contained herein are the private views of the authors and are not to be construed as official or as reflecting the views of the Department of the Army or the Department of Defense.

DOI: 10.1097/SHK.0b013e31821d60a4

Report Documentation Page

Form Approved
OMB No. 0704-0188

1. REPORT DATE	2. REPORT TYPE	3. DATES COVERED
01 AUG 2011	**N/A**	**-**

4. TITLE AND SUBTITLE	5a. CONTRACT NUMBER
Wood bark smoke induces lung and pleural plasminogen activator inhibitor 1 and stabilizes its mRNA in porcine lung cells	5b. GRANT NUMBER
	5c. PROGRAM ELEMENT NUMBER
6. AUTHOR(S)	5d. PROJECT NUMBER
Midde K. K., Batchinsky A. I., Cancio L. C., Shetty S., Komissarov A. A., Florova G., Walker III K. P., Koenig K., Chroneos Z. C., Allen T.,	5e. TASK NUMBER
	5f. WORK UNIT NUMBER
7. PERFORMING ORGANIZATION NAME(S) AND ADDRESS(ES)	8. PERFORMING ORGANIZATION REPORT NUMBER
United States Army Institute of Surgical Research, JBSA Fort Sam Houston, TX	
9. SPONSORING/MONITORING AGENCY NAME(S) AND ADDRESS(ES)	10. SPONSOR/MONITOR'S ACRONYM(S)
	11. SPONSOR/MONITOR'S REPORT NUMBER(S)

12. DISTRIBUTION/AVAILABILITY STATEMENT
Approved for public release, distribution unlimited

13. SUPPLEMENTARY NOTES

14. ABSTRACT

15. SUBJECT TERMS

16. SECURITY CLASSIFICATION OF:			17. LIMITATION OF ABSTRACT	18. NUMBER OF PAGES	19a. NAME OF RESPONSIBLE PERSON
a REPORT	b ABSTRACT	c THIS PAGE			
unclassified	**unclassified**	**unclassified**	**UU**	**10**	

and regulation of PAI-1 in the progression of SIALI has been limited. This represents an important gap in our current understanding of the pathogenesis of SIALI. *In vivo* and *in vitro* approaches were applied to address this gap.

We used a porcine model of wood bark smoke (WBS)–induced ALI to determine whether robust expression of PAI-1 is induced in the lungs and whether its distribution occurs in proximity to extravascular fibrin *in situ*. We also sought to determine whether WBS components induce expression of PAI-1 by resident lung cells *in vitro*. In these analyses, we first tested the ability of WBS extracts to induce PAI-1 in early primary cultures of porcine lung alveolar type II (ATII) cells, lung fibroblasts, and pleural mesothelial cells (PMCs). Next, we sought to shed light on the mechanism by which PAI-1 is induced in these cells by WBS. We specifically sought to determine whether the mechanism involves stabilization of PAI-1 mRNA, as it is well established that PAI-1 is regulated at the transcriptional level by mediators likely to be operative in SIALI (8, 13). Understanding of the role of posttranscriptional regulation of PAI-1 in this context or in any other form of ALI has not, to our knowledge, previously been studied and is addressed here.

MATERIALS AND METHODS

Animals

This study was approved by the US Army Institute of Surgical Research Animal Care and Use Committee and was carried out in accordance with the guidelines set forth by the Animal Welfare Act and other federal statutes and regulations relating to animals and studies involving animals and by the 1996 *Guide for the Care of Laboratory Animals* from the National Research Council. For this study, we enrolled a randomly selected subset of swine that were part of a larger study evaluating the efficacy of conventional mechanical ventilation versus airway pressure release ventilation (APRV) for treatment of SIALI. A total of 22 female, nonpregnant, Yorkshire pigs (35 45 kg) were used in this study. Lung tissues from eight of animals not subjected to BAL were used for histologic and immunohistochemical analyses exclusively. Of these eight animals, five were killed at 48 h after induction of SIALI and two at 24 h after SIALI, whereas one served as a mechanically ventilated time control (over 48 h). Fourteen additional animals were subjected to BAL, and tissues were obtained for histologic analyses. Of these 14 animals, 12 underwent WBS challenge, whereas two served as mechanically ventilated time controls. Three of these 12 WBS challenged animals did not develop ARDS, whereas the other nine pigs developed SIALI over 48 h. The pigs were premedicated, anesthetized, intubated, and mechanically ventilated using a Dräger Evita XL ventilator (Dräger Medical, Lübeck, Germany) in a volume controlled mode with a baseline setting of tidal volume (TV) of 10 mL/kg, a positive end expiratory pressure (PEEP) of 5 cm H_2O, an inspiratory to expiratory ratio of 1:3, and fraction of inspired oxygen (F_{IO_2}) of 21%. At baseline (before injury), the partial pressure of carbon dioxide (P_{ACO_2}) was maintained between 35 and 45 mmHg by adjusting the respiratory rate. Arterial, venous, and pulmonary artery and urinary bladder catheters were placed for physiologic monitoring. A tracheostomy was performed, to maintain a safe airway during smoke inhalation and subsequent intensive care unit (ICU) care.

Physiologic monitoring

Pigs were monitored for 48 h. The following variables were measured: number of smoke breaths received, volume of smoke received, peak carboxy hemoglobin level after smoke injury, peak inspiratory pressure, partial pressure of O_2 in arterial blood (P_{AO_2}), partial pressure of CO_2 in arterial blood (P_{ACO_2}), fraction of inspired oxygen (F_{IO_2}), and P_{AO_2} to F_{IO_2} ratio (PFR). Data were recorded at baseline (before injury) and every 6 h thereafter for 48 h.

WBS inhalation

After a 45 to 90 minute stabilization period baseline (preinjury), physiologic values were obtained, after which the animals were taken to a room for administration of WBS (14). Briefly, 100 g of pine wood bark chips was burned in a custom combustion chamber. Room air was blown through the chamber, and the smoke was vented into a mixing box for cooling to avoid thermal injury. Next, the smoke/air/oxygen mixture was drawn into a volume controlled, hand operated piston and delivered to the animals via a tracheostomy. Tidal volume per smoke breath was set at 30 mL/kg, and smoke was delivered as described in Table 1. Smoke injury was terminated if the pig developed hemodynamic instability, manifested by severe hypotension or desaturation during the injury.

ICU care

After injury, pigs were transported to the animal ICU, where they remained under round the clock clinical monitoring for 48 h under total intravenous anesthesia with ketamine hydrochloride (20 30 mg/kg per hour), midazolam hydrochloride (1.0 1.5 mg/kg per hour), and propofol (50 100 μg/kg per minute). Analgesia was provided with buprenorphine (0.05 mg/kg i.m.) every 6 h. For 2 h after injury, a F_{IO_2} of 100% was used to accelerate carbon monoxide clearance. After 2 h, the F_{IO_2} was tapered to 21% and titrated to an arterial oxygen saturation greater than 92%. Suctioning was performed as needed. Fiberoptic bronchoscopy was performed at baseline, immediately after injury, and every 6 h during the first 24 h; then at 24 and 48 h. This served to remove any major obstructing casts and to carry out BAL as described in the following sections.

Mechanical ventilation protocols

Before injury, pigs exposed to WBS were randomized to receive either conventional mechanical ventilation (CMV) using volume assist control (n = 12) or APRV (n = 7). Three of the WBS challenged animals ventilated with CMV did not develop severe hypoxemia within 2 h, whereas all other pigs required 100% oxygen supplementation, consistent with the development of SIALI. For 2 h after injury, F_{IO_2} of 100% was used to accelerate carbon monoxide clearance; other ventilator settings continued as at baseline with a TV = 10 mL/kg, respiratory rate = 12 breaths/min, and PEEP = 5 cm H_2O. After 2 h, F_{IO_2} was tapered down to 21% and was subsequently titrated to achieve an arterial oxygen saturation greater than 92%. At that time, pigs were either continued on CMV or transitioned to APRV. A plateau pressure less than 35 mmHg was sought in both the CMV and APRV arms. In the CMV arm, the respiratory rate (up to a rate of 30), followed by the TV, was adjusted to achieve $7.5 > pH_a > 7.2$. In the APRV arm, the P_{high} and T_{low} were adjusted to maintain $7.5 > pH_a > 7.2$. Uninjured time control pigs (n = 3) were maintained on CMV at TV = 10 mL/kg, PEEP = 5 cm H_2O, and F_{IO_2} = 21%. Pigs in all three groups received humidification in the ventilator circuit.

BAL protocol

Bronchoalveolar lavage was performed at baseline and at 24 and 48 h after injury. Control BAL fluid (BALF) was obtained at the same intervals in mechanically ventilated pigs not challenged with WBS. The bronchoscope was gently wedged in a subsegmental bronchus (in the accessory lobe on the left), and 20 mL of normal saline solution was instilled and gently aspirated. The procedure was repeated three times, recording the yield after each instillation.

TABLE 1. **Smoke inhalation data**

Mode	Weight, kg	Smoke breaths, n	Smoke, L	Peak COHb, %
CMV (n 9)	42.31 ± 1.55	22.44 ± 1.67	27.44 ± 3.59	80.88 ± 2.10
APRV (n 7)	41.51 ± 1.36	23.29 ± 1.63	28.58 ± 2.31	86.70 ± 1.63
P	0.31	0.73	0.81	0.05

Inhalation injury data in the CMV and APRV groups with SIALI, indicating injury equivalency. Values are means ± SEMs. Significance by two-tailed Student *t* test or Wilcoxon two-sample test.
Peak COHb indicates peak carboxyhemoglobin concentration at end of smoke injury by arterial blood gas analysis.

The cells were removed by centrifugation at 400*g* for 10 min, after which cell free fluids were frozen at 70°C until analyzed.

Experimental termination, necropsy, and specimen collection

All animals that survived 48 h after injury received a euthanasia solu tion (Fatal Plus; Med Vet International, Mettawa, Ill) in accordance with the AVMA Guidelines on Euthanasia, June 2007.

Collection and propagation of primary cultures of ATII cells, lung fibroblasts, and PMCs

Porcine ATII epithelial cells were harvested at necropsy and isolated by modifications of a previously described protocol (15). Excised porcine lung tissue was cut in 1 mm pieces with the aid of a tissue chopper and fine scissors. Each isolation involved use of 20 to 25 g of tissue. Chopped tissue was shaken vigorously at 250 revolutions per minute in 100 mL of Ca^{++}, Mg^{++} free Hanks balanced salt solution (HBSS) and at 37°C for 5 min. Tissue fragments were then filtered three times over a 100 μm nylon mesh to remove red blood cells. Washed tissue was with 15 mL of an enzymatic solution containing 50 U/mL Dispase I (BD Pharmingen cat. no. 354235, San Diego, Calif) supplemented with 2,000 U/mL DNAse I (Sigma cat. no. D5025, St. Louis, Mo). The tis sue was then digested for 45 min at 37°C in a water bath shaker at 125 revolu tions per minute. The enzymatic reaction was stopped with 20 mL of Dulbecco modified Eagle medium (DMEM)/10% fetal bovine serum (FBS). Undigested tissue was then removed by sequential filtration over 100 and 40 μm cell strainers (Fisher Scientific, Freemont, Calif). Filtrates were then centrifuged at 250*g*, 10°C for 20 min. Cell pellets were resuspended in erythrocyte lysis buf fer (0.5 mL/g tissue digested) and incubated at room temperature for 4 min. An equal volume of Dulbecco modified Eagle medium/10% FBS was then added, and cells were recovered by centrifugation at 250*g*, 10°C for 20 min. The cells were washed in 20 mL of Ca^{++}, Mg^{++} free HBSS resuspended in alveolar epi thelial cell medium (ScienCell cat. no. 3201, Carlsbad, Calif) supplemented with 10 U/mL DNAase I and cultured in a 75 cm^2 tissue culture plate for 1 h at 37°C in a humidified 95% air/5% CO_2 incubator to adhere macrophages. Nonadherent cells were removed, centrifuged as above, and resuspended in alveolar epithelial cell medium. Epithelial cells were isolated by Percoll density gradient cen trifugation as described previously (15). The Percoll density gradient consisted of two layers: a light upper layer at Percoll density of 1.040 g/mL and a lower heavy layer at a density of 1.089 g/mL in Ca^{++}, Mg^{++} free HBSS supplemented with 0.05% FBS. Epithelial cells were harvested from the interface using after centrifugation at 250*g* for 30 min at 10°C, diluted in 20 mL of Ca^{++}, Mg^{++} replete HBSS, washed twice by centrifugation, and cultured in 25 cm^2 tissue culture plates for 48 h. The cells were harvested using 0.05% trypsin/0.5 mM EDTA (Invitrogen, Carlsbad, Calif), washed, and stored frozen at 80°C in cell freezing medium (ScienCell cat. no. 0133) until use. Pleural mesothelial cells were cultured from citrated (3.8% sodium citrate in a 1:9 vol:vol ratio) pleural fluids (PFs) from the injured pigs and placed on ice, and PMCs and lung fibro blasts were harvested and characterized with minor modifications of the techni ques we previously reported (16). Alveolar type II cells and PMCs used in these studies were successfully harvested from the lungs (n = 3 animals) and PF (n = 1/ 18 cultures attempted) from pigs at 48 h after SIALI. Lung fibroblasts were harvested from lungs of ventilated control pigs (n = 2) and from animals or 48 h after SIALI (n = 8).

Preparation of WBS extract

Pine bark wood chips were combusted in a conical flask. The smoke gen erated was collected and passed into phosphate buffered saline (PBS) through a peristaltic pump attached. An optical density of 1 at 230 nm was considered 100%, and fresh WBS extract (WBSE) was made 30 min before each use. The WBSE was sterilized through a 0.2 μm filter and diluted with appropriate media to the desired concentration before application to primary cells in culture.

Western and polymerase chain reaction analyses

Western blotting of BAL and conditioned media was done as we previously described (17). Plasminogen activator inhibitor 1 was detected using rabbit polyclonal PAI 1 AB (Abcam 28207, Cambridge, Mass). The PAI 1 standard was from American Diagnostica (Greenwich, Conn; no. 1092). Total RNA was isolated from cultured porcine primary cells by using Tri reagent. Five micro grams of total RNA was reverse transcribed for 45 min at 42°C using reverse transcriptase polymerase chain reaction (PCR) kit from Promega (Madison, Wis). Plasminogen activator inhibitor 1 and β actin mRNA were amplified for over 30 cycles using porcine specific primers along with $P^{[32]}$ dCTP. The for ward porcine PAI 1 primer was 5′ ATT GCT CCT CTC TTT TCC TTG 3′. The reverse primer was 5′ TCA TTT TCT CTC CCT CTC TCA C 3′. The PCR product was separated using a 5% urea gel, autoradiographed over night, and normalized to β actin for quantification of PAI 1 mRNA.

Fibrin-plate radioassay, fibrin enzymography, and reverse fibrin enzymography

The fibrinolytic capacity of BALF was determined in a fibrin plate assay in which the release of radiolabeled fibrin was measured, as we previously re ported (7). The fibrinolytic activity of BAL was further characterized by fibrin enzymography, a technique in which BAL samples were subjected to sodium dodecyl sulfate polyacrylamide gel electrophoresis (SDS PAGE) after which zones of fibrinolytic activity were detected on a fibrin gel underlay, as we pre viously reported (7). Reverse enzymography was used to identify zones of PAI activity, as previously reported (7).

Proteins and reagents

Plasminogen, plasmin (PL), and fluorogenic PL substrate were purchased from Haematologic Technologies Inc (HTI, Essex Junction, Vt). Specific synthetic fluorogenic urokinase PGN activator (uPA) and chromogenic PL substrates were from Centerchem (Norwalk, Conn). Concentrations of proteins were calculated with a BCA protein assay kit (Pierce, Rockford, Ill).

Measurement of uPA and PL amidolytic activity

Amidolytic uPA and PL activity was determined from time traces of changes in the fluorescence emission at 440 and 470 nm, respectively (exci tation, 344 and 352 nm, respectively) of fluorogenic uPA (Pefafluor uPA; Centerchem Inc, Norwalk, Conn) or fluorogenic PL (HTI) substrates, respec tively, in 0.1 M HEPES buffer (pH 7.4, 20 mM NaCl). Aliquots (5 20 μL) of samples were mixed with buffer (total volume, 50 μL) in 96 well white flat bottom Costar plates (Corning Inc, Corning, NY). Equal volumes of 0.1 mM Pefafluor uPA or 0.2 mM PL substrates in the same buffer were added and mixed. Increases in fluorescence emission were detected using a Varian Cary Eclipse fluorescence spectrophotometer equipped with 96 well plate reader accessory (Varian Inc, Walnut Creek, Calif). A linear equation was fit to the results using Varian software. Enzymatic activities were reported as arbitrary units (AUs) calculated based on tcuPA (American Diagnostica, Stamford, Conn) and PL (HTI) standards. Plasminogen activation was measured as a difference between endogenous PL activity of the BAL sample and increasing PL activity, which was generated due to activation of exogenous human PGN (0.2 1 μM) added to the sample. Plasminogen was purchased from HTI. Amidolytic uPA, PL, and PGN activation activity was analyzed using Varian Eclipse Kinetic Software (Varian Inc). The quality of the fit was estimated by visual analysis of plots of the residuals (deviation of the fitted function from the actual data). Statistical significance and medians and values at 75% and 25% intervals were determined using the Mann Whitney rank sum test as described previously (18). $P < 0.05$ was considered statistically significant. Box plots of the results of measuring uPA, PL, PGN activating, and fibrinolytic activity were generated as previously described (18) using SigmaPlot 11.0 and SigmaStat 3.5 software (SPSS Inc, San Jose, Calif).

Assessment of apoptosis

Apoptotic cells were detected in lung tissues of ventilated control pigs and those with SIALI by TUNEL staining, as we previously reported (19).

Transcription chase analyses

The determination of the effects of WBSE on PAI 1 mRNA stability was per formed as we previously reported (19). In these analyses, ongoing transcription was stopped after which the stability of the PCR amplified transcripts of cells exposed to WBSE was compared with that of control vehicle exposed cells.

Gel shift and UV cross-linking analyses

The interaction of a newly characterized PAI 1 mRNA binding protein with its cognate 33 nucleotide (nt) 3′ UTR binding sequence on PAI 1 mRNA was tested as we recently reported (20). The fibroblasts used in these analyses were derived from control ventilated pigs to maximize the opportunity to visualize differences in the binding interaction in control versus WBSE or TGF β.

Histologic, immunohistochemical, and morphometric analyses

Formalin fixed right lower lobe tissue was used for histologic and immu nohistochemical analyses. All 24 lung tissues from pigs surviving 24 or 48 h after treatment and lungs from control untreated, ventilated pigs were pro cessed and examined. Pig lungs were sectioned grossly, and sections contain ing pleura, lung parenchyma, small airways, and conducting airways were placed into paraffin blocks. Five micron sections from each pig lung block were placed on glass slides, stained with hematoxylin eosin (H&E), and cover slipped H&E scores were interpreted as previously described (17). One hun dred high power fields per slide were examined in morphometric analyses (400×, except for large and small airway fibrin at 100×). Lung injury score was calculated on the H&E slides as follows: atelectasis or edema 0 = none;

TABLE 2. **Acute lung injury scoring**

Mode	Atelectasis	Fibrin			Alveolar septal inflammatory cell infiltrate	Alveolar edema
		ALV	SA	LA		
CMV (n 9)	0.89 ± 0.26*	2.67 ± 0.17†	2.22 ± 0.15†	1.78 ± 0.28†	2.56 ± 0.29†	1.56 ± 0.29
APRV (n 7)	1.86 ± 0.14‡	3.00 ± 0‡	2.71 ± 0.18‡	2.00 ± 0.22‡	2.86 ± 0.14‡	2.14 ± 0.40
CTRL (n 3)	0.67 ± 0.33	0	0	0	0	0.67 ± 0.33

Ventilatory modes are as defined in Materials and Methods.
LA scoring for each parameter: 0 none present; 1 involvement <25% of the field; 2 25% 50% involvement; 3 >75% involvement. Hematoxylin-eosin stained sections of the lung (n 22) were examined by a pathologist with specialized training in lung pathology (TA). 100 high-power-field (400×) sections were examined in each to assess alveolar fibrin deposition and inflammation in each case, and SA and LA involvement was assessed by scanning the sections at medium (100×) power. Means ± SEs are shown.
*$P < 0.05$ CMV versus APRV.
†$P < 0.05$ CMV versus CTRL.
‡$P < 0.05$ APRV versus CTRL.
ALV indicates alveolar; CTRL, control mechanically ventilated pigs; LA, large airway; SA, small airway.

1 = mild airspace atelectasis or edema (<25% of airspaces affected); 2 = moderate airspace atelectasis or edema (25% 75% of airspaces affected); and 3 = severe airspace atelectasis or edema (>75% of airspaces affected); inflammation 0 = no alveolar/interstitial inflammatory infiltrate; 1 = mild alveolar/interstitial inflammatory cell infiltrate (no or minimal septal thicken ing, involving <25% of alveoli and interstitium); 2 = moderate interstitial chronic inflammatory cell infiltrate (minimal septal thickening involving 25% to 75% of the alveoli and interstitium; 3 = severe interstitial inflammatory cell infiltrate including septal thickening involving more than 75% of the alveoli and interstitium. Fibrin immunostained lung sections from control and 24 or 48 h post SIALI pigs were scored as follows: fibrin 0 = no fibrin; 1 = fibrin involving less than 25% of large, small or alveolar spaces; 2 = fibrin involving 25% to 75% of the same airspaces; 3 = fibrin involving more than 75% of air spaces. Immunohistochemical analyses for detection of fibrin and PAI 1 were performed using antibodies directed against the human proteins, as we previously described (17). In immunohistochemical analyses for p53, antibody sc 98 (Santa Cruz Biotechnology, Santa Cruz, Calif) was used as the primary antibody.

Statistical analysis

For physiologic analyses, all values expressed are means ± SEM. Statistical analyses were performed using SAS 9.1 software, Cary, NC: two way ANOVA with repeated measures and Tukey Kramer adjustment for multiple comparisons, when appropriate, as well as two tailed Student *t* test or Wilcoxon two sample test. Significance was accepted at $P < 0.05$. Non normally distributed data were log transformed before analysis.

RESULTS

WBS exposure and physiologic derangements confirming induction of ALI

All animals with SIALI, whether subjected to CMV or APRV, received comparable smoke exposure as indicated by the number of breaths, the volume of smoke, and the peak

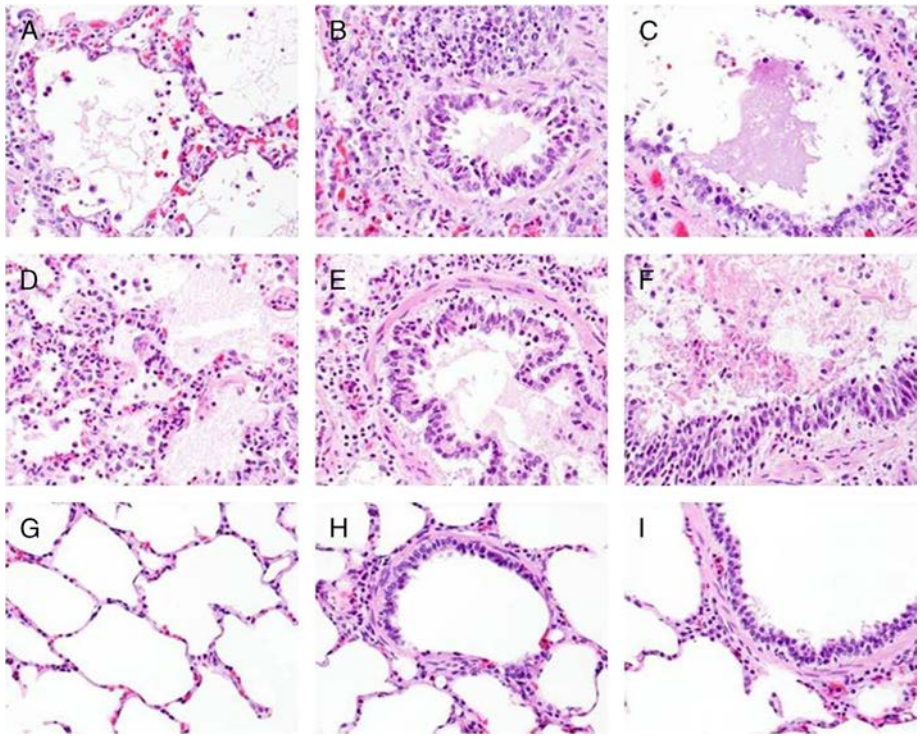

FIG. 1. **Histology of SIALI in porcine lung tissue**. Lung sections were fixed as described in Materials and Methods and stained with H&E. Images representative of the findings in the lungs of control ventilated pigs or those with SIALI are illustrated at 400× magnification. Comparison of alveoli, small airways, and large airways in representative APRV and CMV ventilated animals (48 h) and in ventilated controls (48 h) shows similar fibrin deposition in alveoli (arrows) and alveolar septal chronic inflammation in the APRV and CMV ventilated animals (A and D, respectively) and essentially normal alveoli in the ventilated control animal (G). Small airways and large airways in the APRV and CMV ventilated animals (B and E, and C and F, respectively) show fibrin deposition within airways, whereas the small airways and large airways in the ventilated control animal (H and I, respectively) demonstrate no fibrin deposition.

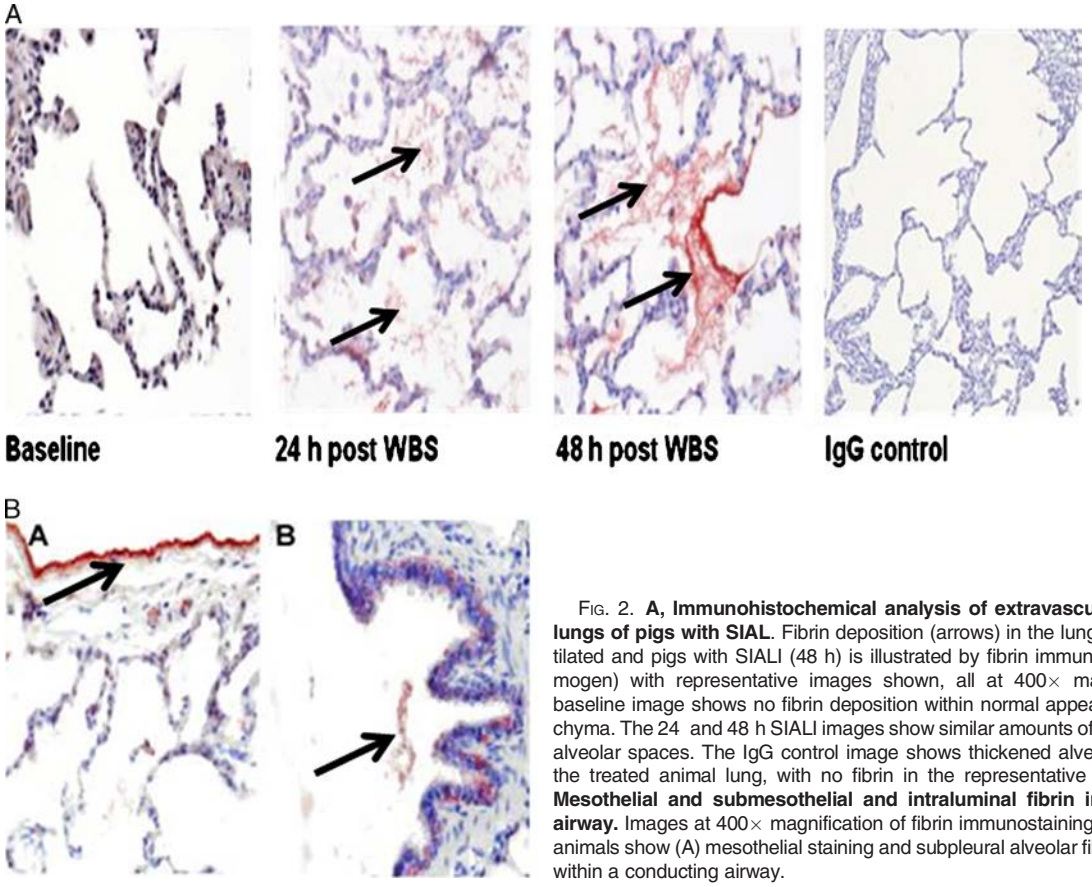

FIG. 2. **A, Immunohistochemical analysis of extravascular fibrin in the lungs of pigs with SIAL**. Fibrin deposition (arrows) in the lungs of control ventilated and pigs with SIALI (48 h) is illustrated by fibrin immunostain (red chromogen) with representative images shown, all at 400× magnification. The baseline image shows no fibrin deposition within normal appearing lung parenchyma. The 24 and 48 h SIALI images show similar amounts of fibrin lying within alveolar spaces. The IgG control image shows thickened alveolar septa within the treated animal lung, with no fibrin in the representative control slide. **B, Mesothelial and submesothelial and intraluminal fibrin in a conducting airway.** Images at 400× magnification of fibrin immunostaining (arrows) of 48 h animals show (A) mesothelial staining and subpleural alveolar fibrin and (B) fibrin within a conducting airway.

carboxyhemoglobin concentration (Table 1). By 24 h after injury, peak inspiratory pressure was significantly increased in animals with SIALI (36 cm H_2O) versus time controls (18 cm H_2O; $P < 0.05$). From 30 to 48 h after injury, the PFR was significantly lower in injured animals (PFR, 139) than in controls (PFR, 440; $P < 0.05$).

Histologic and morphometric assessment of SIALI

We initially characterized the extent and distribution of acute inflammation, alveolar edema, and extravascular fibrin deposition in pigs with evolving SIALI. The histologic appearance of SIALI did not differ between animals that succumbed early at 24 h (n = 2; one ventilated with CMV, the other with APRV) versus those that survived for 48 h (n = 14), nor in pigs maintained on CMV versus APRV, with the exception that animals ventilated with CMV demonstrated significantly less focal atelectasis versus those ventilated with APRV (Table 2). All animals exposed to WBS demonstrated histologic evidence of ALI except for three animals ventilated with CMV that did not develop gas exchange abnormalities indicative of ARDS. These three animals uniformly demonstrated grade 1 fibrin deposition but otherwise did not exhibit histologic changes that differed from mechanically ventilated controls (n = 3). At 24 h after WBS exposure, alveolar edema was prominent with irregular foci of alveolitis. At 48 h after induction of ALI by WBS, the histologic appearance of SIALI

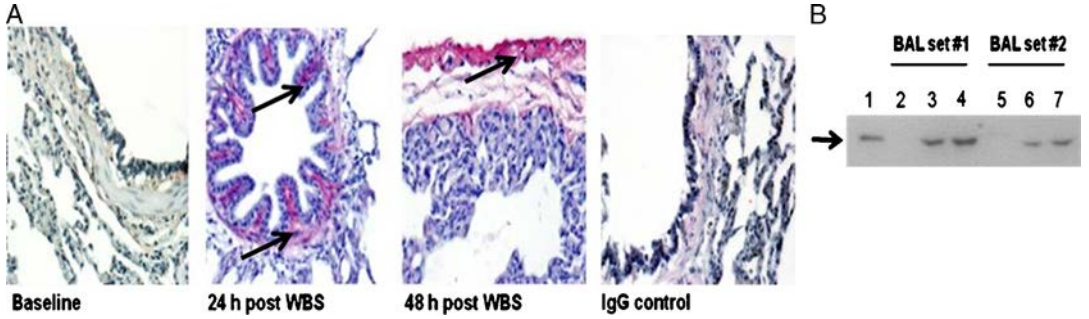

FIG. 3. **Identification of PAI-1 in lung tissues of control pigs and those with SIALI**. A, Plasminogen activator inhibitor 1 staining was not detectable in the lungs of control ventilated animals. Immunopositivity for PAI 1 antigen was detectable in the peribronchial tissues at 24 h after injury. Strong immunopositivity for PAI 1 antigen was detectable in the mesothelium and in subpleural connective tissues at 48 h after injury. Arrows indicate areas of immunoreactivity. IgG represents negative control to show the typical extent of background staining (400×) (data representative of sets from n = 3 animals)). B, Western blot analysis of porcine BAL for PAI 1 expression. Lane 1: recombinant PAI 1 standard (10 ng) is illustrated. Lanes 2 and 5: BAL from before injury. Lanes 3 and 6: BAL from animals harvested at 24 h after injury. Lanes 4 and 7: BAL 48 h after injury. Data illustrated are representative of those analyzed from serially obtained BALs (n = 6 animals).

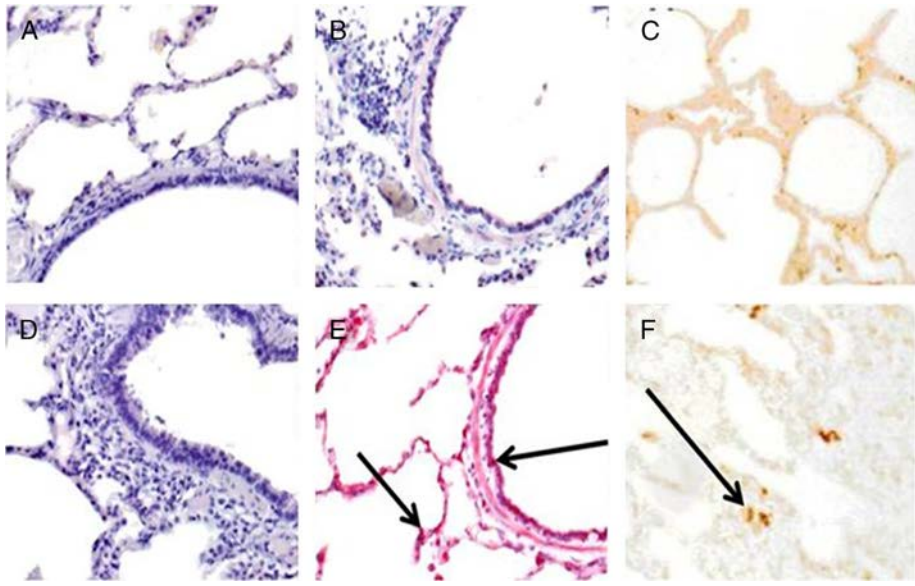

FIG. 4. **p53 expression and apoptosis is increased in the interstitial tissues in SIALI**. Immunohistichemical staining of representative lung tissue images from control lungs (panels A C) and those from pigs with SIALI at 48 h (panels D F, n = 3 animals/group) for p53. Strong p53 staining was seen in the airway epithelium and alveolar interstitium (arrows) at 48 h after SIALI (E) versus control lung tissue (B). No staining was detectable with control IgG in each of the tissues (panels A and D). Histologic examination of TUNEL stained slides of porcine lungs revealed negative immunonegative staining in the control animals (panel C) and strong nuclear positivity indicative of apoptotic change in the interstitium and lung parenchyma of animals with SIALI at 48 h (n = 3/group, panel F). Images are shown at 400× magnification.

was characterized by florid alveolar edema, which appeared to contain fibrinous debris, interstitial edema, hyaline membrane formation, and alveolitis, which involved a prominent neutrophilic component (Fig. 1, B–D) and fibrinous airway casts (Fig. 1E). We found no evidence of lung edema or acute inflammation in the lungs of the control animals (n = 3), whereas patchy areas of atelectasis were observed in all of these cases. There was no evidence of dense neutrophilic infiltrates characteristic of bronchopneumonia in any of the pigs (n = 22).

We next used immunohistochemistry to confirm the presence of airway fibrin in animals with established SIALI. Extravascular fibrin deposition was not detectable in the lung parenchyma of time-control pigs over 48 h (Fig. 2, baseline left panel). As anticipated, there was florid alveolar fibrin deposition at 24 and 48 h after injury (Fig. 2A). The small airways were also involved. As described in Materials and Methods, large airway casts were removed by bronchoscopy, but fibrin was identified within some conducting airways in 48-h animals (Fig. 2B). Using two independent analyses in which we used either a monoclonal antibody against human fibrinogen or a rabbit polyclonal antibody to murine fibrinogen, we confirmed that fragments of large airway casts exhibited diffuse reactivity and therefore contained fibrin (Fig. 2E). No reactivity was demonstrated in controls exposed to the respective IgG primary antibodies (Fig. 2A, rightmost panel). By morphometric analyses performed in all controls and randomly selected 24 h pigs (n = 3/group) and three randomly selected 48-h SIALI animals, fibrin was demonstrated in the alveoli and small airways of the lungs of pigs with SIALI. Scores for alveoli, small airways, and conducting airways were, respectively, 0/0/0 for baseline animals. In the alveoli, the scores alveolar and small airway fibrin deposition were uniformly 3 and 2 for 24- and 48-h pigs (n = 3/group), whereas conducting airway fibrin was less frequent with a morphometric score of 1 in one 24-h animal and two 48-h animals and 0 in the others.

As PAI-1 has been strongly implicated in extravascular fibrin maintenance and in the progression of other forms of ALI (6), we next sought to establish that this inhibitor was likewise expressed proximate to areas of fibrin deposition in

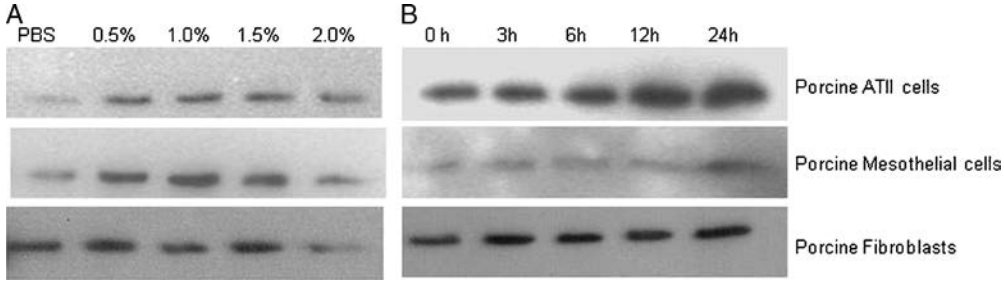

FIG. 5. **Dose (A) and time course (B) responses of the induction of PAI-1 expression in primary porcine lung cells exposed to WBS extract**. Induction of PAI 1 antigen in primary porcine PMCs, ATII cells, and lung fibroblasts exposed to WBS extract *in vitro*. A, Dose responses: Conditioned media from porcine primary cells exposed to different doses of WBS extract (WBSE) for 24 h and resolved by 10% SDS PAGE gel. The separated proteins were then transferred to a nitrocellulose membrane followed by PAI 1 antigen detection using rabbit polyclonal PAI 1. B, Time course experiments: 50 μL of conditioned media from porcine cells exposed to 1.0% WBSE in a time dependent manner was analyzed for PAI 1 antigen by Western blotting. The blots in each case are representative of the findings in duplicate independent experiments.

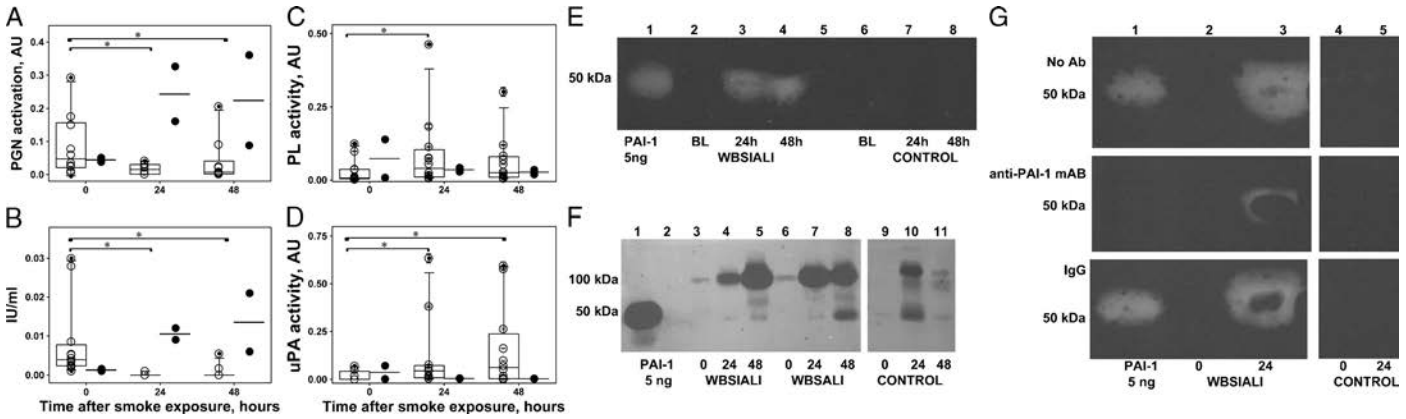

FIG. 6. **Plasminogen Activator and Fibrinolytic Activities and PAI-1 Expression in BAL of Animals with SIALI**. A, A box plot of changes in PA activity with time. Plasminogen activity (expressed in AUs) was determined in BAL of animals before (0 h) and after (24 and 48 h) induction of SIALI (n = 9, including four pigs ventilated with CMV and five with APRV); each value shown as a circle (ventilated controls [n = 2] are shown in dark circles). Statistically significant differences ($P < 0.05$) are indicated with asterisks (all samples done in duplicate analyses). B, A box plot of changes in the fibrinolytic activity as determined by release of radiolabeled fibrin in the same samples. Fibrinolytic activity was expressed in international units (IU) per mL of BAL. C and D, Changes in plasmin and urokinase amidolytic activities (expressed in AUs) determined in the same BAL samples. E, Reverse fibrin enzymography representative of the findings in BAL samples of all nine 48 h SIALI and two control uninjured, mechanically ventilated pigs, showing the appearance of zones of resistance to fibrinolytic activity in BAL after ALI and absence of these bands in the BAL of timed control pigs. F, Enzymographic analysis representative of the BAL findings in 48 h SIALI pigs (n = 9) and controls (n = 2), showing increased PA PAI 1 complexes at 100 kd after injury. Zones of free uPA activity were also detectable in control and injured animals. G, Neutralization of zones of resistance to fibrinolysis in BAL of animals with SIALI by impregnation of the indicator gel with an antibody to human PAI 1 in reverse enzymographic analyses.

SIALI. Focal mucosal and submucosal PAI-1 expression was noted in the large and small airways of pigs with SIALI at 24 and 48 h (Fig. 3A). The same animals were used for morphometric assessment of the distribution of PAI-1. Faint PAI-1 was detectable in the alveolar walls of all animals (n = 3/group), whereas strong staining for PAI-1 was demonstrable in the submucosal areas of the airways of pigs with SIALI (Fig. 3A). Plasminogen activator inhibitor 1 expression was readily detected in BAL of pigs with SIALI (Fig. 3B), likely because PAI-1 is secreted by lung epithelial cells. Strong staining for PAI-1 was observed in the mesothelium and subpleural connective tissues (Fig. 3A).

In further analyses, we found that SIALI was further characterized by prominent interstitial apoptosis (Fig. 4). Apoptotic cells were identified predominantly in alveolar septae. In selected instances, the apoptotic cells appeared to be alveolar and airway epithelial cells. As p53 has been strongly implicated in apoptosis of resident lung cells, we also sought to determine the distribution of this tumor suppressor in the lungs of pigs with SIALI exposed to WBS for 24 or 48 h and control pigs (n = 3/group). In lung tissues at 24 or 48 h after induction of SIALI, p53 expression was prominent in the airway epithelium, in submucosal tissues of the airways, vascular smooth muscle, and in the alveoli (not shown).

Based on the immunohistochemical demonstration of PAI-1 induction in evolving SIALI, we next sought to determine if exposure of primary resident porcine lung cells to components of WBS was capable of inducing PAI-1. To this end, we isolated primary lung ATII cells, lung fibroblasts, and PMCs from porcine lung tissue or PFs and exposed the cells to WBSE after which PAI-1, a secreted protein, was measured in the conditioned media. Cells exposed to the extract vehicle served as negative controls. In initial dose-response analyses (Fig. 5A), we found that exposure of each of these cell types to WBSE for 24 h induced PAI-1, with maximal induction occurring at a concentration of 0.5% to 1.5%. In time-course analyses (Fig. 5B), exposure of ATII cells, lung fibroblasts, and PMCs to 1% WBSE was found to induce maximal expression of PAI-1 in the conditioned media after 24 h of exposure. The responses of fibroblasts cultured from control ventilated pigs and those at 48 h after SIALI were comparable in these analyses (not shown). These experiments confirm that cultured porcine ATII cells, lung fibroblasts, and PMCs uniformly respond to WBSE with induction of PAI-1.

We next used amidolytic, fibrin-plate, and enzymographic analyses to confirm that PAI-1 activity is expressed in BAL and, in particular, by PMCs (Fig. 6), which exhibited robust expression of PAI-1 (Fig. 3A). We found that BAL PGN activator (PA) activity and ability to lyse fibrin were both significantly decreased by 24 or 48 h after induction of SIALI

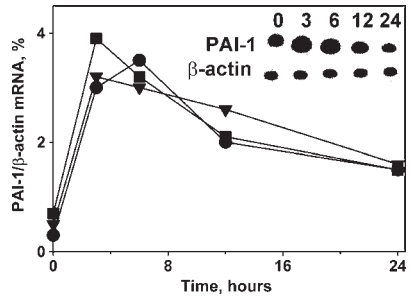

FIG. 7. **Time dependence of PAI-1 mRNA expression in primary porcine cells exposed to 1.0% WBS extract**. Total RNA was isolated by phenol chloroform extraction after the indicated time intervals. Five micrograms of total RNA was subjected to RT PCR for 45 min at 42°C. The reverse transcribed product was PCR amplified for 30 cycles using porcine PAI 1 and β actin primers followed by separation of the PCR product on 5.0% urea gel. The gel was later dried for 2 h and autoradiographed overnight at 80°C. The densitometric ratios of PAI 1/β actin mRNA were plotted over time as illustrated in the line graph (● = epithelial cells, ▼ = mesothelial cells, ■ = fibroblasts). The gel image represents the maximal PAI 1 mRNA induction at 3 h in PMCs. The plotted densitometric data are representative of three independent experiments in PMCs, ATII cells, and lung fibroblasts.

(Fig. 6, A and B). Interestingly, relatively low levels of BAL PL and uPA activity were detectable at 24 and 48 h (Fig. 6, C and D). There were no significant differences for any of the parameters illustrated in Figure 6, A–D, between the CMV and APRV groups. Although BALs from only two ventilated controls were available, a trend of preserved PA and fibrinolytic activity in BAL was observed over 48 h. Depressed BAL fibrinolytic activity at 24 and 48 h appeared to be, at least in part, suppressed by increased PAI-1. This was shown by reverse fibrin enzymography (Fig. 6E), showing increased formation of PA-PAI-1 complexes (Fig. 6F). Zones of resistance to PA activity were inhibited by an antibody to PAI-1 impregnated in the indicator gel, indicating that the PAI we identified was, in fact, PAI-1 (Fig. 6G).

In complementary studies, we assessed the time course of induction of PAI-1 mRNA in these cells by PCR analyses (Fig. 7). As shown in the densitometric plots of PAI-1 mRNA normalized to the expression of β-actin mRNA (Fig. 7), PAI-1 mRNA was induced in ATII cells, lung fibroblasts, and PMCs at 3 to 6 h after exposure to 1% WBSE for 24 h. These analyses demonstrate that the induction of PAI-1 mRNA precedes that of the induction of the protein in resident porcine lung cells.

Although PAI-1 expression is well known to be regulated at the transcriptional level, we recently reported that it was controlled at the level of PAI-1 mRNA stability in PMCs (20). We next blocked ongoing transcription and found that PAI-1 mRNA was stabilized in primary porcine ATII cells, lung fibroblasts, and PMCs exposed to 1% WBSE for 24 h compared with PBS-treated cells (Fig. 8). This is visualized in a densitometric plot of PAI-1 mRNA normalized to β-actin mRNA (Fig. 8). These analyses confirm that these cell types respond to WBSE exposure with stabilization of PAI-1 mRNA. These studies also indicate that increased stability of PAI-1 mRNA contributes to the induction of PAI-1 in each of these cell types and strongly suggest that the process could be operative in SIALI *in vivo*.

Lastly, we sought to further elucidate the mechanism by which PAI-1 mRNA was regulated in porcine lung cells. Given the limited availability of ATII cells, lung fibroblasts, and PMCs, analyses were by necessity restricted to elucidation of the posttranscriptional control of PAI-1 expression. Using gel-shift and UV cross-linking analyses, we were able to detect an interaction between PAI-1 mRNA binding protein and PAI-1 mRNA in porcine PMCs, lung fibroblasts, and ATII cells (Fig. 9). The interaction involves a PAI-1 mRNA binding protein that, like human 6-phospho-D-gluconate-NADP oxidoreductase (6-PGD), migrates at about 60 kd (20). Exposure of each of these cell types to 1% WBSE for 24 h disrupted the binding protein–PAI-1 mRNA interaction (Fig. 9, lanes 2, 5, 8, and 11), as did treatment of the cells with transforming growth factor β (TGF-β) (lanes 3, 6, 9, and 12). The response to TGF-β recapitulates the responses of human pleural mesothelial and lung epithelial cells, as we recently reported (20), and shows that MeT5A cells (lanes 1–3) respond to WBSE with dissociation of the regulatory complex as they do to TGF-β. Because we assessed the binding of putative porcine PAI-1 mRNA binding interactions using a 33-nt transcript known to bind the PAI-1 mRNA destabilizing protein 6-PGD, we can conclude that the binding interaction we observed here involves a porcine 6-PGD –like protein.

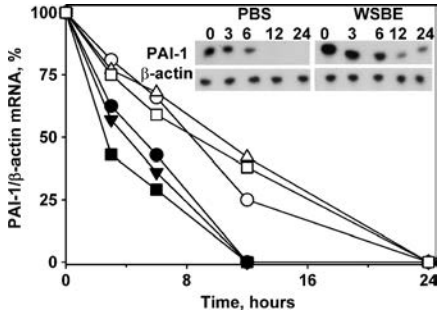

FIG. 8. **Stability of PAI-1 mRNA is increased after WBSE exposure: transcription chase experiments**. Porcine primary cells were exposed to PBS (filled symbols) or 1.0% WBSE (empty symbols) for 3 h, followed by blocking ongoing transcription with DRB (20 μg/mL) and actinomycin (5 μg/mL) at the indicated time intervals. Total RNA was isolated and reverse transcribed as described earlier. The densitometric ratios of PAI 1/β actin mRNA stabi lized after DRB treatment were plotted over time as shown in the line graph (circles epithelial cells, triangles mesothelial cells, squares fibroblasts). The gel image is representative of PAI 1 mRNA stabilization after DRB treat ment in primary porcine PMCs.

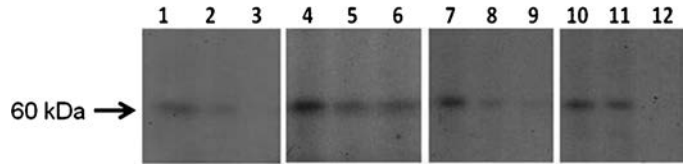

FIG. 9. **The PAI-1 mRNA and PAI-1 mRNABP dissociates in primary PMCs, ATIIs and lung fibroblasts after exposure to 1.0% WBS Extract or TGF-b**. One hundred micrograms of total cellular protein from porcine primary cells treated with 1.0% WBSE for 24 h was hybridized with ^{32}P d[UTP] 33 nt PAI 1 mRNA transcript for 30 min. The sample was then incubated with RNAse for 30 min at 37°C and heparin for 10 min at room temperature. The samples were then UV cross linked at 2,500 J for 45 min on ice followed by separation of the mixture on 10% SDS PAGE at 35 V. The gels were later dried and autoradiographed overnight at 80°C to detect the PAI 1 mRNA binding protein. Arrow indicates the binding interaction (representing the 60 kd 6 PGD like PAI 1 mRNA binding protein [PAI 1 mRNABp]). Lanes 1 3: PAI 1 mRNA PAI 1 mRNA BP interaction in MeT5A human PMCs exposed to buf fer, 1.0% WBSE (lane 2) or 2 ng/mL TGF β (lane 3) over 24 h. Lanes 4 6: Porcine PMCs; lanes 7 9: porcine ATII cells; lanes 10 12: porcine fibroblasts (same format; n = 1 3 independent experiments per cell type). Free probe is not shown.

DISCUSSION

We found that extravascular fibrin is florid in this porcine model of SIALI and that it is distributed in the conducting airways as well as in the small airways and alveolar space. Although clinical inhalation injury involves variable exposure to a complex mixture of particulates and toxic gases, this model reliably generates inhalationally induced ALI that exhibits key features of the clinical disease. Airway casts that form within 24 h after induction of SIALI were confirmed to be fibrinous by immunohistochemical analyses. The prominent fibrinous casts in the conducting airways likely contribute to the increased airway resistance often observed in SIALI induction of bronchospasm initiated by coagulation in the airways as previously been reported in SIALI. This may be attributable to intraluminal deposition of airway fibrin (21). In our model, bronchoscopic removal of these casts was mandatory for survival of animals challenged with SIALI, which

may have limited their detection in conducting airways of tissues harvested at necropsy. Prominent alveolar fibrin deposition likely contributes to the surfactant dysfunction, atelectasis, and impaired gas exchange that characterize this model and that are known to occur in clinical SIALI.

Our data indicate that PAI-1 is induced in the lungs in SIALI and that increased PAI-1 is temporally associated with and proximate to sites of extravascular fibrin deposition. Plasminogen activator inhibitor 1 was found to be induced in the epithelium and connective tissues of the airways and in the subpleural connective tissues and mesothelium within 24 to 48 h after injury. In addition, PAI-1 expression was increased in BAL of pigs during the progression of SIALI over this same time frame, indicating that small airway and alveolar lining fluids were enriched. By fibrin-plate analyses, fibrinolytic activity was detectable in the BAL of control animals and relatively decreased in that of pigs with SIALI, indicating that induction of PAI-1 was at least in part responsible for the defect in local fibrinolytic activity in BAL. Despite evidence of relatively low levels of uPA and PL amidolytic activities in BAL, the presence of concurrently increased PAI-1 was demonstrated by reverse enzymography and likely accounts for much of the decrement of PA activity in amidolytic analyses. These results could indicate formation of "molecular cage"–type complexes between macroglobulins and uPA and PL, which we detected in PFs of animals with pleural injury (18). Collectively, these data confirm that PAI-1 contributes to the decreased fibrinolytic activity observed in BAL of pigs with SIALI, promotes persistence of airway and alveolar fibrin deposition, and thereby contributes to abnormal gas exchange observed in this model. We found that removal of fibrinous large airway casts by bronchoscopy improved gas exchange and decreased peak airway pressure, suggesting that this approach may likewise be of lifesaving value in patients with SIALI, especially those with evidence of large airway obstruction and atelectasis.

Because parenchymal lung expression of PAI-1 was robust in SIALI, as shown by immunohistochemical analyses, we inferred that resident lung cells would substantively contribute to PAI-1 expression if challenged with components of WBS. To address this possibility, we isolated and tested the ability of WBSE to induce PAI-1 in porcine ATII cells, lung fibroblasts, and PMCs by Western blot and PCR analyses. Interestingly, we found that WBSE induced PAI-1 secretion by all of these resident lung cells and that the magnitude of the response was comparable. As PAI-1 is a secreted protein, ATII cells and lung fibroblasts may contribute to the levels of PAI-1 seen in BAL after induction of SIALI, and PAI-1 is likewise induced in PMCs. Although it is likely that the cells harvested from the lungs of the SIALI animals were activated, our data clearly show that they retain the ability to increase PAI-1 in response to WBSE exposure.

We next sought to test the mechanism by which WBSE induced PAI-1. It is well known that PAI-1 gene expression is regulated at the level of transcriptional activation by mediators that, like TGF-β, are present in the setting of high-grade inflammation (13). To our knowledge, however, there have been no prior studies that addressed the possibility that PAI-1 is regulated at the level of posttranscriptional control of mRNA stability in this context. We recently reported that lung epithelial cells and PMCs regulate PAI-1 at the posttranscriptional level (20), providing us with a strong rationale to investigate whether this pathway is operative in SIALI. In that study, we reported a novel PAI-1 mRNA destabilizing interaction involving the interaction of PAI-1 mRNA with a protein we characterized as 6-PGD. Transforming growth factor β−mediated induction of PAI-1 was found to dissociate 6-PGD from its specific 33-nt binding sequence within 3′ UTR of PAI-1 mRNA. In the present study, we report, for the first time, that a similar mechanism is operative when primary porcine PMCs, lung fibroblasts, or ATII cells are stimulated with WBSE or TGF-β. Our group previously showed that PAI-1 may be induced by an alternate mechanism in which induction of PAI-1 in lung epithelial cells of mice with bleomycin-induced ALI or human ATII cells exposed to bleomycin or cigarette smoke extract occurred through interaction of p53 with PAI-1 mRNA (8). Although we found immunohistochemical evidence of induction of p53 and interstitial apoptosis of the lungs of animals with SIALI, we found no evidence of the interaction of p53 with PAI-1 mRNA by gel-shift analysis. It is possible that this finding relates to differences in the interaction of the human PAI-1 mRNA binding sequence with porcine p53. Our findings are consistent with the immunohistochemical findings indicating that PAI-1 is induced in these cell types in SIALI and suggest the likely possibility that the process could contribute to PAI-1 expression in the airways, alveoli, and mesothelium in pigs with SIALI.

Our observations confirm that SIALI exhibits profound impairment of the pulmonary fibrinolytic system and that PAI-1 overexpression contributes to the effect. These changes are characteristic of ALI (8), but their contribution to the pathogenesis of ALI appears to be complex. For example, lung function is not altered in PAI-1 or fibrinogen knockout mice with ALI induced by hydrochloric acid (22), but the authors acknowledge that the effects of hydrochloric acid on surfactant and lung dysfunction do not obviate the potentially important effects of locally increased PAI-1 and fibrin deposition in ALI on altered microvascular permeability, inflammatory cell recruitment, lung remodeling, or subsequent fibrotic repair. These derangements may have special relevance to clinical SIALI, because fibrinous airway casts are a prominent feature not usually seen in other forms of ALI. It is of interest that fibrinolytic therapy has successfully been used to clear the intravascular clots and fibrinous transitional matrix and to reverse respiratory dysfunction in various forms of ALI, in swine and in patients with ARDS (23, 24). To mitigate the risk of systemic bleeding, nebulized therapy with tissue PA has more recently been used and was found to reverse pulmonary dysfunction when instituted early (within 4 h) in SIALI (3). Aerosolized anticoagulants were also shown to be beneficial in SIALI but were initiated even earlier (within 2 h of inhalation injury) in sheep (4). These studies provide proof of principle that localized intervention that targets airway and alveolar fibrin is salutary. These studies raise the possibility that this or other relatively PAI-1–resistant agents such as single-chain urokinase (scuPA) (17) could be of advantage when delivered

by inhalation in SIALI. We found that activity of scuPA is protected from inactivation by PAI-1 in BALF of pigs with SIALI (not shown), which suggests that the mechanism of protection recapitulates that which occurs in PFs—where scuPA or two-chain uPA form complexes with α_2 macroglobulin (18).

In conclusion, PAI-1 is induced in the lungs of swine with wood bark smoke–induced ALI. The increment of PAI-1 in the airways, mesothelium, and alveoli is concurrently associated with decreased BAL fibrinolytic activity and promotes extravascular fibrin in these locations. Overexpression of PAI-1 in the airways likely sustains intrabronchial fibrin casts, which are amenable to clearance by inhalational interventions that target fibrin deposition. Wood bark smoke extract induces PAI-1 expression in primary ATII cells, lung fibroblasts, and PMCs *in vitro*. This strongly suggests that these cells may all contribute to PAI-1 expression in this model. The induction mechanism involves stabilization of PAI-1 mRNA in ATII cells and PMCs. This study represents the first demonstration of this mode of regulation of PAI-1 in this or any other form of ALI.

ACKNOWLEDGMENTS

The authors thank Bryan Jordan, MSN; Michael Lucas; Corina Necsoiu, MD; and Ruth Nguyen MD, for their technical and administrative support.

REFERENCES

1. Enkhbaatar P, Traber DL: Pathophysiology of acute lung injury in combined burn and smoke inhalation injury. *Clin Sci (Lond)* 107(2):137 143, 2004.
2. Demling RH: Smoke inhalation lung injury: an update. *Eplasty* 8:e27, 2008.
3. Enkhbaatar P, Murakami K, Cox R, Westphal M, Morita N, Brantley K, Burke A, Hawkins H, Schmalstieg F, Traber L, et al.: Aerosolized tissue plasminogen inhibitor improves pulmonary function in sheep with burn and smoke inhalation. *Shock* 22(1):70 75, 2004.
4. Enkhbaatar P, Cox RA, Traber LD, Westphal M, Aimalohi E, Morita N, Prough DS, Herndon DN, Traber DL: Aerosolized anticoagulants ameliorate acute lung injury in sheep after exposure to burn and smoke inhalation. *Crit Care Med* 35(12):2805 2810, 2007.
5. Murakami K, McGuire R, Cox RA, Jodoin JM, Bjertnaes LJ, Katahira J, Traber LD, Schmalstieg FC, Hawkins HK, Herndon DN, et al.: Heparin nebulization attenuates acute lung injury in sepsis following smoke inhalation in sheep. *Shock* 18(3):236 241, 2002.
6. Idell S: Coagulation, fibrinolysis, and fibrin deposition in acute lung injury. *Crit Care Med* 31(suppl 4):S213 S220, 2003.
7. Idell S, James KK, Levin EG, Schwartz BS, Manchanda N, Maunder RJ, Martin TR, McLarty J, Fair DS: Local abnormalities in coagulation and fibrinolytic pathways predispose to alveolar fibrin deposition in the adult respiratory distress syndrome. *J Clin Invest* 84(2):695 705, 1989.
8. Shetty S, Padijnayayveetil J, Tucker T, Stankowska D, Idell S: The fibrinolytic system and the regulation of lung epithelial cell proteolysis, signaling, and cellular viability. *Am J Physiol Lung Cell Mol Physiol* 295(6):L967 L975, 2008.
9. Sapru A, Curley MA, Brady S, Matthay MA, Flori H: Elevated PAI-1 is associated with poor clinical outcomes in pediatric patients with acute lung injury. *Intensive Care Med* 36(1):157 163, 2010.
10. Tsangaris I, Tsantes A, Bonovas S, Lignos M, Kopterides P, Gialeraki A, Rapti E, Orfanos S, Dimopoulou I, Travlou A, et al.: The impact of the PAI-1 4G/5G polymorphism on the outcome of patients with ALI/ARDS. *Thromb Res* 123(6):832 836, 2009.
11. Prabhakaran P, Ware LB, White KE, Cross MT, Matthay MA, Olman MA: Elevated levels of plasminogen activator inhibitor-1 in pulmonary edema fluid are associated with mortality in acute lung injury. *Am J Physiol Lung Cell Mol Physiol* 285(1):L20 L28, 2003.
12. Aoki K, Aikawa N, Sekine K, Yamazaki M, Mimura T, Urano T, Takada A: Elevation of plasma free PAI-1 levels as an integrated endothelial response to severe burns. *Burns* 27(6):569 575, 2001.
13. Dimova EY, Kietzmann T: Metabolic, hormonal and environmental regulation of plasminogen activatorinhibitor-1 (PAI-1) expression: lessons from the liver. *Thromb Haemost* 100(6):992 1006, 2008.
14. Park MS, Cancio LC, Batchinsky AI, McCarthy MJ, Jordan BS, Brinkley WW, Dubick MA, Goodwin CW: Assessment of severity of ovine smoke inhalation injury by analysis of computed tomographic scans. *J Trauma* 55(3):417 427, 2003.
15. Murphy SA, Dinsdale D, Hoet P, Nemery B, Richards RJ: A comparative study of the isolation of type II epithelial cells from bat, hamster, pig and human lung tissue. *Methods Cell Sci* 21(1):31 38, 1999.
16. Shetty S, Idell S: A urokinase receptor MRNA binding protein from rabbit lung fibroblasts and mesothelial cells. *Am J Physiol* 274(6 pt 1):L871 L882, 1998.
17. Idell S, Allen T, Chen S, Koenig K, Mazar A, Azghani A: Intrapleural activation, processing, efficacy, and duration of protection of single-chain urokinase in evolving tetracycline-induced pleural injury in rabbits. *Am J Physiol Lung Cell Mol Physiol* 292(1):L25 L32, 2007.
18. Komissarov AA, Mazar AP, Koenig K, Kurdowska AK, Idell S: Regulation of intrapleural fibrinolysis by urokinase-alpha-macroglobulin complexes in tetracycline-induced pleural injury in rabbits. *AM J Physiol Lung Cell Mol Physiol* 297(4):L568 L577, 2009.
19. Shetty S, Shetty P, Idell S, Velusamy T, Bhandary YP, Shetty RS: Regulation of plasminogen activator inhibitor-1 expression by tumor suppressor protein P53. *J Biol Chem* 283(28):19570 19580, 2008.
20. Shetty S, Velusamy T, Shetty RS, Marudamuthu AS, Shetty SK, Florova G, Tucker T, Koenig K, Shetty P, Bhandary YP, et al.: Posttranscriptional regulation of plasminogen activator inhibitor-1 expression in human pleural mesothelial cells. *Am J Respir Cell Mol Biol* 43(3):358 367, 2009.
21. Wagers SS, Norton RJ, Rinaldi LM, Bates JH, Sobel BE, Irvin CG: Extravascular fibrin, plasminogen activator, plasminogen activator inhibitors, and airway hyperresponsiveness. *J Clin Invest* 114(1):104 111, 2004.
22. Allen GB, Cloutier ME, Larrabee YC, Tetenev K, Smiley ST, Bates JH: Neither fibrin nor plasminogen activator inhibitor-1 deficiency protects lung function in a mouse model of acute lung injury. *Am J Physiol Lung Cell Mol Physiol* 296(3):L277 L285, 2009.
23. Hardaway RM, Williams CH, Marvasti M, Farias M, Tseng A, Pinon I, Yanez D, Martinez M, Navar J: Prevention of adult respiratory distress syndrome with plasminogen activator in pigs. *Crit Care Med* 18(12):1413 1428, 1990.
24. Hardaway RM, Harke H, Williams CH: Fibrinolytic agents: a new approach to the treatment of adult respiratory distress syndrome. *Adv Ther* 11(2):43 51, 1994.